NEURAL REGENERATION RESEARCH
www.nrronline.org

Research Article

Identification of injury type using somatosensory and motor evoked potentials in a rat spinal cord injury model

Rong Li[1, 2], Han-Lei Li[3], Hong-Yan Cui[3], Yong-Can Huang[4], Yong Hu[1, 5, *]

https://doi.org/10.4103/1673-5374.346458
Date of submission: September 25, 2021
Date of decision: January 14, 2022
Date of acceptance: April 25, 2022
Date of web publication: June 2, 2022

From the Contents

Graphical Abstract

The change patterns of SEPs and MEPs can reflect SCI induced by different mechanical mechanisms

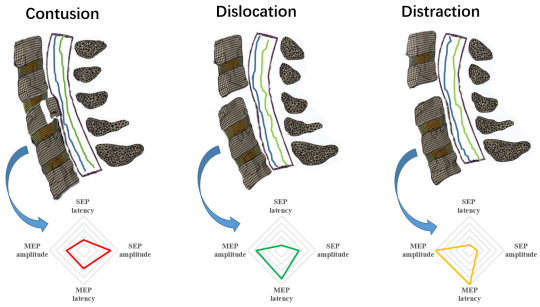

Abstract

The spinal cord is at risk of injury during spinal surgery. If intraoperative spinal cord injury is identified early, irreversible impairment or loss of neurological function can be prevented. Different types of spinal cord injury result in damage to different spinal cord regions, which may cause different somatosensory and motor evoked potential signal responses. In this study, we examined electrophysiological and histopathological changes between contusion, distraction, and dislocation spinal cord injuries in a rat model. We found that contusion led to the most severe dorsal white matter injury and caused considerable attenuation of both somatosensory and motor evoked potentials. Dislocation resulted in loss of myelinated axons in the lateral region of the injured spinal cord along the rostrocaudal axis. The amplitude of attenuation in motor evoked potential responses caused by dislocation was greater than that caused by contusion. After distraction injury, extracellular spaces were slightly but not significantly enlarged; somatosensory evoked potential responses slightly decreased and motor evoked potential responses were lost. Correlation analysis showed that histological and electrophysiological findings were significantly correlated and related to injury type. Intraoperative monitoring of both somatosensory and motor evoked potentials has the potential to identify iatrogenic spinal cord injury type during surgery.

Key Words: contusion injury; dislocation injury; distraction injury; electrophysiology; heterogeneity; histopathology; injury mechanism; motor evoked potential; somatosensory evoked potential; spinal cord injury

Introduction

Spinal cord injury (SCI) is heterogeneous in terms of injury location, injury type, and extent of neurologic impairment at the time of presentation (Tator, 2006; Choi et al., 2021; Ghasem-Zadeh et al., 2021). Rescue measures differ for different types of SCI. Choo et al. (2007) compared histological changes in the acute injury phase between three types of SCI and found that dislocation and contusion resulted in extensive hemorrhage and membrane compromise, whereas distraction injury was characterized by longer longitudinal membrane disruption without detectable hemorrhage. In a rat SCI model, contusion, dislocation, and distraction injuries exhibited distinct histopathological changes and behavioral recovery (Chen et al., 2016; Tian et al., 2021; Chen and Li, 2022). Moreover, the pattern of secondary spinal cord degeneration varies according to injury type, indicating that treatment for different although clinically-related injuries may ultimately require targeted neuroprotective strategies (Choo et al., 2008). Identification of SCI type is important because SCI type has significant treatment implications.

Spinal surgery carries the risk of iatrogenic SCI. Although *in vitro* histological and functional analyses have revealed important SCI pattern details, the various patterns are difficult to distinguish and apply to diagnosis since they do not yield real-time information. Integrated monitoring of somatosensory-evoked potentials (SEPs) and motor-evoked potentials (MEPs) has been advocated as an essential tool to assess functional integrity of the spinal cord during spine surgery (MacDonald et al., 2019; Nuwer and Schrader, 2019). A previous report suggested abnormal changes in SEPs and MEPs can be detected early in ischemic SCI (Kakinohana et al., 2007). Other studies have shown that both are lost rapidly in contusion injuries and gradually after compression injury (Morris et al., 2017; Huang et al., 2018). Dislocation injury mainly affects SEP amplitude rather than latency (Mattucci et al., 2019). A comprehensive analysis of SEP and MEP signal characteristics may allow differentiation of SCI type. In this study, we aimed to examine and compare electrophysiological and histopathological changes between contusion, distraction, and dislocation injuries in a rat model. Furthermore, we evaluated evoked potentials as a predictor of injury type. We hypothesized that different SCI injury types have distinct patterns of evoked potential signal change.

Methods

Animals

All procedures were conducted in accordance with the Care and Use of Laboratory Animals guidelines (Institute of Laboratory Animal Resources,

[1]Department of Orthopedics and Traumatology, The University of Hong Kong-Shenzhen Hospital, Shenzhen, Guangdong Provinve, China; [2]Department of Neurosurgery, Neuroscience Center, Integrated Hospital of Traditional Chinese Medicine, Southern Medical University, Guangzhou, Guangdong Provinve, China; [3]Institute of Biomedical Engineering, Chinese Academy of Medical Sciences and Peking Union Medical College, Tianjin, China; [4]Shenzhen Engineering Laboratory of Orthopedic Regenerative Technologies, Department of Spine Surgery, Peking University Shenzhen Hospital, Shenzhen, Guangdong Provinve, China; [5]Department of Orthopedics and Traumatology, The University of Hong Kong, Pokfulam, Hong Kong Special Administrative Region, China
*Correspondence to: Yong Hu, PhD, yhud@hku.hk.
https://orcid.org/0000-0003-0305-5616 (Yong Hu)

Funding: *This work was supported by the National Natural Science Foundation of China, No. 81871768 (to YH); Natural Science Foundation of Tianjin, China, No. 18JCYBJC29600 (to HYC); and High Level-Hospital Program, Health Commission of Guangdong Province, China, No. HKUSZH201902011 (to YH).*
How to cite this article: *Li R, Li HL, Cui HY, Huang YC, Hu Y (2023) Identification of injury type using somatosensory and motor evoked potentials in a rat spinal cord injury model. Neural Regen Res 18(2):422-427.*

National Research Council, 1996). The study was approved and supervised by the Research Ethics Committee at Peking University Shenzhen Hospital (approval No. 2017-004) on August 26, 2017. Thirty-nine male Sprague-Dawley rats (specific-pathogen-free level, aged 7 to 8 weeks, weight 280 to 320 g) were purchased from Guangdong Medical Laboratory Animal Center (license No. SCXK (Yue) 2018-0002) and randomly assigned to contusion (n = 10), dislocation (n = 10), and distraction (n = 10) injury groups and three sham groups (n = 3, respectively).

SCI models

Animals were anesthetized for SCI, evoked potential testing, and sacrificed using intraperitoneally injected pentobarbital sodium (60 mg/kg; Sigma, St. Louis, MO, USA) and xylazine (10 mg/kg; Sigma). The injury level was located between T12 and T13. Using standard aseptic principles and techniques, the thoracolumbar spine was surgically exposed. Customized vertebral clamps were used to rigidly hold the transverse processes of T11, T12, T13, and L1. Spinal cord function was continuously monitored using SEPs and MEPs to ensure no accidental damage occurred prior to injury. The rats were placed on a thermostatic pad at 37°C to receive a subcutaneous injection of 5 mL physiological saline solution to prevent dehydration. Contusion, distraction, and dislocation injuries were performed between T12 and T13 (**Figure 1**).

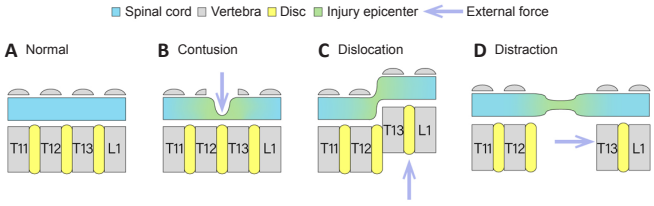

Figure 1 | **Schema of normal spinal cord and contusion, dislocation, and distraction spinal cord injury mechanisms.**
(A) Normal spinal cord. (B) To generate contusion, a laminectomy was performed and the dorsal spinal cord was impacted vertically between T12 and T13 using a flat, 2 mm diameter tip. (C) For dislocation injury, T12–T13 facetectomy was performed and dislocation was performed using an actuator coupled with vertebral clamps to apply an external dorsal displacement of the T12 vertebral body relative to T13. (D) For distraction injury, the vertebral clamps were used to apply distraction between T12 and T13 after the facetectomy.

Contusion injury was created by spinal cord displacement using the NYU-MASCIS impact system (Rutgers, New Brunswick, NJ, USA) as previously reported (Wang et al., 2015). Briefly, a small circular laminectomy was performed to expose the spinal cord dura between T12 and T13 (**Figure 1B**). Stabilization clamps were used to immobilize the T12 and T13 vertebrae during impact. The injury was produced by dropping a 10 g rod from a height of 20 mm onto the exposed dural surface. For dislocation injury, dorsal ligament resection and facet arthrotomy were performed at the T12–T13 interspace. The T11 and T12 vertebrae were fixed using customized vertebral clamps, while another clamp was tightly connected to the T13 and L1 vertebrae. T13 and L1 were dorsally dislocated by 2 mm and then returned to the initial position (**Figure 1C**). To model distraction injury, the T12–T13 facets were removed and clamps coupled to a distraction apparatus were placed on T11/T12 and T13/L1. The respective clamps were distracted rostrally and caudally to produce a displacement of 3 mm and held for 1 second before being returned to their initial position (**Figure 1D**). The sham groups received identical surgical procedures except for injury induction.

Neuroelectrophysiological assessment

Immediately after SCI, electrophysiological evaluation (YRKJ-G2008; Yirui Technology Co., Ltd., Zhuhai, China) was conducted as described in our previous study (Hu et al., 2011). SEP latency was defined as the time from stimulation to the maximum negative deflection. Amplitude was measured as the maximum voltage between the peak of the positive and negative deflections.

Tibial SEPs were evoked from stimulation proximal to the ankle via a pair of needle electrodes (NE-S-1500/13/0.4; Friendship Medical Electronics Co., Ltd., Xi'an, China) using the following parameters: 0.1 ms duration, 5.3 Hz frequency, and 3–5 mA intensity (to elicit mild toe twitching). Recordings were collected using two scalp needle electrodes subcutaneously inserted over the primary somatosensory cortex and a frontal midline reference electrode. Signals were averaged over 500 responses and filtered between 30 and 3000 Hz.

For MEPs, constant current stimulation was applied to the motor cortex using two needle electrodes (0.1 ms duration, 300 Hz frequency, 30–50 mA intensity). MEPs were recorded from the gastrocnemius muscle using needle electrodes. The signals were band-pass filtered at a frequency from 30 to 3000 Hz.

Latency measures the time to onset of SEP waveform in response to stimulation. Amplitude measures the peak-to-peak intensity of SEP waveform. Latency extension is presented as (L1 – L0)/L0 where L0 indicates baseline latency and L1 indicates postoperative latency. Amplitude reduction is presented as (A0 – A1)/A0 where A0 indicates baseline latency and A1 indicates postoperative latency.

Histological analysis

The influence of different primary injury types on spinal cord histopathology was assessed immediately after electrophysiological assessment. Transcardial perfusion was performed approximately 20 minutes after SCI in all animals with 200 mL 0.01M phosphate-buffered saline followed by 300 mL of 4% paraformaldehyde. Spinal cord samples 10 mm in length containing the lesion epicenter were collected, placed overnight in 4% paraformaldehyde, and cryoprotected in graded concentrations of sucrose (12%, 18%, 24% in phosphate-buffered saline). Samples were sequentially cross sectioned at a thickness of 20 µm for histology and divided equally into 10 sets of sections at 200 µm intervals.

One set of spinal cord slides was stained with hematoxylin and eosin for analysis of overall injury distribution and hemorrhage (Huang et al., 2018). Briefly, slides were rinsed in distilled H_2O, stained with hematoxylin, differentiated in 1% aqueous HCl, and then counterstained with eosin. Sections were dehydrated in ethanol and xylene and coverslipped with mounting medium.

Luxol fast blue (LFB) staining was performed on another set of slides to examine white matter myelination after SCI (Walker et al., 2016). Briefly, slides were dehydrated with graded ethanol. Each section was then placed in LFB solution at 65°C for 2 to 3 hours and differentiated using 0.05% lithium carbonate. Then, sections were washed with distilled water until the desired staining level was achieved. Finally, sections were dehydrated and coverslipped in xylene-based mounting medium.

Immunofluorescence preparation was performed as previously described (Schumacher et al., 2000). Sections were blocked in normal donkey serum (1:10, Jackson ImmunoResearch Laboratories, Baltimore, MD, USA, Cat# 017-000-121, RRID: AB_2337258) for 30 minutes at room temperature and double-stained with purified neurofilament marker against SMI312 (mouse, 1:1000, Biolegend, San Diego, CA, USA, Cat# 837904, RRID: AB_2566782) and myelin basic protein (rabbit, 1:500, Abcam, Cambridge, UK, Cat# ab40390, RRID: AB_1141521) overnight at room temperature in combination with donkey anti-mouse IgG conjugated with DyLight 594 (1:200, Abcam, Cat# 150108, RRID: AB_2732073) and donkey anti-rabbit IgG conjugated with DyLight 488 (1:200, Abcam, Cat# 150073, RRID: AB_2636877) for 2 hours at room temperature. Slides were subsequently washed in phosphate-buffered saline and mounted with Fluorescent Mounting Medium (Cat# ab104135, Abcam).

Hematoxylin and eosin- and LFB-stained tissues were imaged (4× objective lens) under a light microscope (Axioplan 2, Carl Zeiss, Oberkochen, Germany) equipped with a monochrome red, green, and blue wavelength camera. SMI312/myelin basic protein-stained tissues were examined under a fluorescence microscope at 400× magnification (DM4000, Leica, Wetzlar, Germany). Brightness and contrast remained constant for all images in each group section. In each group, select slices at a specific distance from the injury epicenter were used for analysis.

Data processing

Hemorrhage volume was calculated using the Cavalieri method (Howell et al., 2002) with a 50 µm × 50 µm spacing of point probes on sections (15 to 17 per animal) spaced 200 µm apart. Cross-sectional area of the spare tissue and density of myelinated axons were measured in the region of interest (**Figure 2**) using ImageJ software (National Institutes of Health, Bethesda, MD, USA) (Schneider et al., 2012). Electrophysiological data processing was conducted using MATLAB 2016a (MathWorks, Natick, MA, USA).

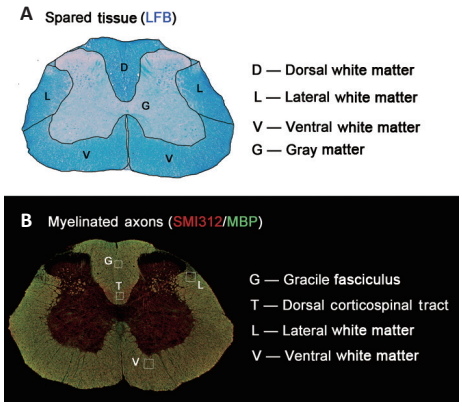

Figure 2 | **Histological regions of interest.**
(A) The lateral, dorsal, and ventral white matter and gray matter were segmented to analyze the residual spinal cord area. (B) Four boxes (100 µm × 100 µm) were placed to compare density of myelinated axons in sections stained with myelin basic protein (MBP) and SMI312. Box locations were middle-right region of the dorsal corticospinal tract, center of the gracile fasciculus, right lateral white matter around the dorsal horn, and right ventral white matter at the edge of the ventral nerve root. LFB: Luxol fast blue.

Statistical analysis

Means were compared between groups using a one-way analysis of variance. With sample sizes of 10 in the three study groups (a total of 30 subjects), the power to detect differences among the means was greater than 95% using an *F* test with 0.05 significance level. No animals or data points were excluded from the analysis. Data of all animals was double-blinded and statistically analyzed using SPSS software version 22.0 (IBM, Armonk, NY, USA). Intergroup differences in the histopathologic data were compared using two-way repeated-measures analysis of variance followed by Tukey's honestly significant difference testing. One-way analysis of variance with Bonferroni *post hoc* testing was used to compare the latency and amplitude of SEP and MEP. Pearson's correlation testing was performed between histological and electrophysiological outcomes. Data are presented as means ± standard deviation. $P < 0.05$ was considered significant.

Results

Electrophysiological differences among different SCI types

Evoked potential waveforms differed between contusion, dislocation, and distraction injuries (**Figure 3**). Different SCI types showed distinct changes in evoked potential patterns (**Figure 4A–D**). Contusion injury resulted in significant latency extension and amplitude reduction in both SEPs and MEPs (**Figure 4B**). Dislocation injury was mainly characterized by MEP deterioration, particularly amplitude attenuation (**Figure 4C**). In distraction injury, SEP amplitude only showed a slight decrease but MEPs disappeared (**Figure 4D**).

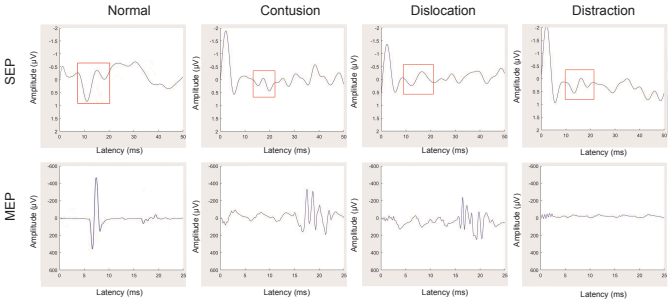

Figure 3 | Representative graphs of evoked potential waveform changes observed with contusion, dislocation, and distraction spinal cord injuries.
SEPs deteriorated in both dislocation and contusion injuries and were slightly reduced in distraction injury. MEPs mainly showed prolonged latency in contusion and dislocation injuries but were abolished after distraction injury. MEP: Motor evoked potential; SEP: somatosensory evoked potential.

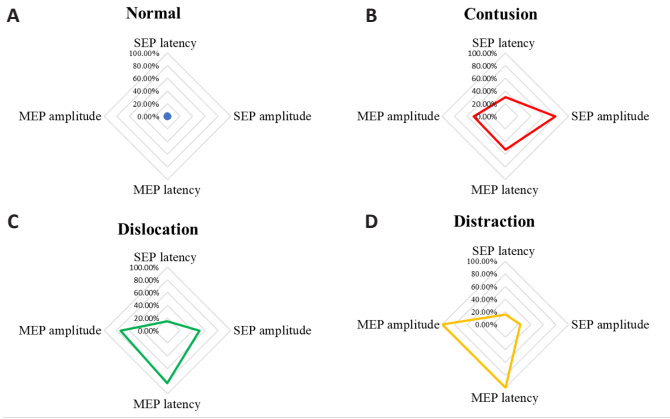

Figure 4 | Time-domain parameters distribution of SEP and MEP amplitude and latency according to type of spinal cord injury.
(A) No significant changes were observed after sham injury. (B) Contusion injury resulted in significant latency extension and amplitude reduction in both SEPs and MEPs. (C) Dislocation injury was mainly characterized by MEP attenuation, particularly decreased amplitude. (D) Distraction injury resulted in a slight reduction in SEP amplitude that was accompanied by loss of MEPs. MEP: Motor evoked potential; SEP: somatosensory evoked potential.

SEP latency was significantly longer in rats with contusion injury (16.22 ± 2.33 ms) than in those with distraction (13.26 ± 1.48 ms, $P = 0.003$) and dislocation (13.67 ± 1.25 ms, $P = 0.002$) injuries. SEP latency was similar in the distraction and dislocation injury groups ($P = 0.459$) and did not significantly differ from SEP latency in the sham group (12.21 ± 0.47 ms, $P = 0.872$ for distraction; $P = 0.378$ for dislocation). Similarly, SEP amplitude was significantly lower in rats with contusion injury (0.41 ± 0.15 μV) than in those with distraction (0.81 ± 0.18 μV, $P = 0.031$) and dislocation (0.89 ± 0.24 μV, $P = 0.001$) injuries. SEP amplitude in the distraction and dislocation injury groups was similar ($P = 0.603$) and significantly lower than SEP amplitude in the sham group (1.65 ± 0.54 μV, $P = 0.025$ for distraction; $P = 0.013$ for dislocation).

Compared with the sham group, MEP onset latency was delayed or absent in the three injury groups (**Figure 3**). Nine of ten rats in the contusion group and eight of ten in the dislocation group exhibited reduced MEP amplitude and prolonged latency; MEP responses were absent in the remaining rats. In all rats of the distraction injury group, MEP responses were absent. Although MEP amplitude significantly differed between the contusion and dislocation injury groups (482.02 ± 94.13 μV *vs.* 245.38 ± 69.18 μV, $P = 0.002$), MEP latency did not (17.12 ± 0.84 ms *vs.* 16.87 ± 0.13 ms, $P = 0.674$). Additional electrophysiological signal change data are reported in **Additional file 1**.

Histological differences among different SCI types

Hemorrhage

Examination of hematoxylin and eosin-stained slides showed extensive primary hemorrhage following contusion or dislocation injuries and slight focal hemorrhage after distraction injury (**Figure 5**). The hemorrhage was concentrated in the gray matter in contusion injury, whereas dislocation injury resulted in hemorrhage in both gray and white matter. Hemorrhage volume in the dislocation (1.04 ± 0.33 mm^3) and contusion (0.98 ± 0.21mm^3) injury groups was similar and significantly larger than hemorrhage volume in the distraction injury group (0.21 ± 0.08 mm^3; **Figure 6**; $P = 0.023$ for dislocation, $P = 0.014$ for contusion).

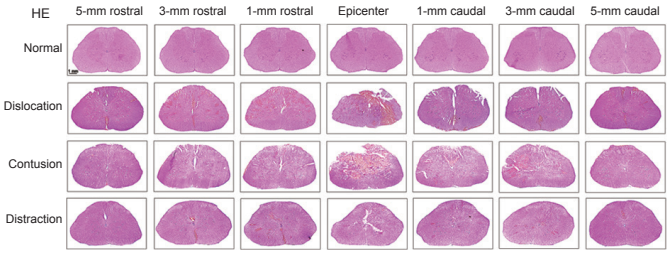

Figure 5 | Representative images showing the asymmetrical rostrocaudal extent of primary hemorrhage after dislocation, contusion, and distraction spinal cord injuries.
Contusion injuries produced concentrated hemorrhage in the gray matter, whereas appreciable hemorrhage was detected in both gray and white matter after dislocation injury. Distraction injury produced minor focal hemorrhage in the white matter. Arrows indicate hemorrhage. Scale bar: 1 mm. HE: Hematoxylin and eosin.

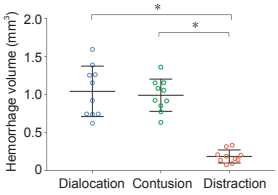

Figure 6 | Primary hemorrhage volume according to type of spinal cord injury.
Hemorrhage volume was similar in contusion and dislocation injuries and significantly lower in distraction injury. Data shown are means ± standard deviation ($n = 10$ in each group). *$P < 0.05$ (two-way repeated-measures analysis of variance followed by Tukey's honestly significant difference testing).

Damage area

Examination of Luxol fast blue-stained slides showed that the rostrocaudal extent of spinal cord disruption was limited to within 3 mm of the injury epicenter in distraction and contusion injuries. For dislocation injuries, laceration was identified 5 mm from the epicenter in some animals (**Figure 7**). Geometrical change was observed in the spinal cord after contusion and dislocation injuries (**Figure 7**). Total cross-sectional area of the spinal cord at the epicenter was smaller in the contusion (5.28 ± 0.37 mm^2, $P = 0.003$) and dislocation injury groups (4.87 ± 0.59 mm^2, $P = 0.001$) than in the sham group (7.12 ± 0.14 mm^2, **Figure 8A**). Compared with the contusion injury group, spinal cords in the dislocation injury group showed greater tissue damage caudal to the lesion site. In contrast, spinal cord cross-sectional area was larger in the distraction injury group (7.06 ± 0.32 mm^2) than in the dislocation and contusion injury groups; however, the area in the distraction injury and sham groups did not significantly differ (**Figure 8A**).

Cross-sectional area of total spared white matter was smaller in the contusion and dislocation injury groups than in the distraction injury and sham groups at the following locations relative to the epicenter of injury (**Figure 8B**): 2.0 mm rostral, 0.6 mm rostral and caudal, 0 mm, and 3.2 mm caudal. The total cross-sectional area of spared white matter was smaller in the dislocation injury group than in the contusion injury group, which was mainly because of a large difference in the dorsal and lateral columns (**Figure 8C** and **D**). In the ventral spinal cord, cross-sectional area of spared white matter surrounding the epicenter did not differ between the sham group and any of the three injury types (**Figure 8E**).

Compared with the sham group, the area of spared gray matter around the epicenter of injury was smaller in both the dislocation and contusion injury groups; the area was smallest in the dislocation injury group (**Figure 8F**). Area of spared gray matter was not significantly different between the distraction injury and sham groups.

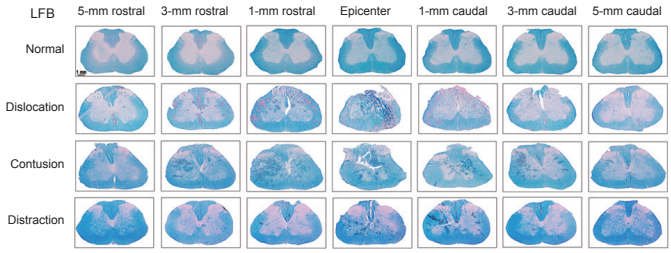

Figure 7 | Representative photomicrographs of Luxol fast blue (LFB)-stained spinal cord sections.
Tissue loss and atrophy as well as fissure injuries were noted on histopathological examination. The lesion extent was limited to 3 mm from the epicenter of injury in distraction and contusion injuries; however, in dislocation injuries, laceration was observed 5 mm rostral and caudal to the epicenter. Arrows indicate tissue loss. Scale bar: 1 mm.

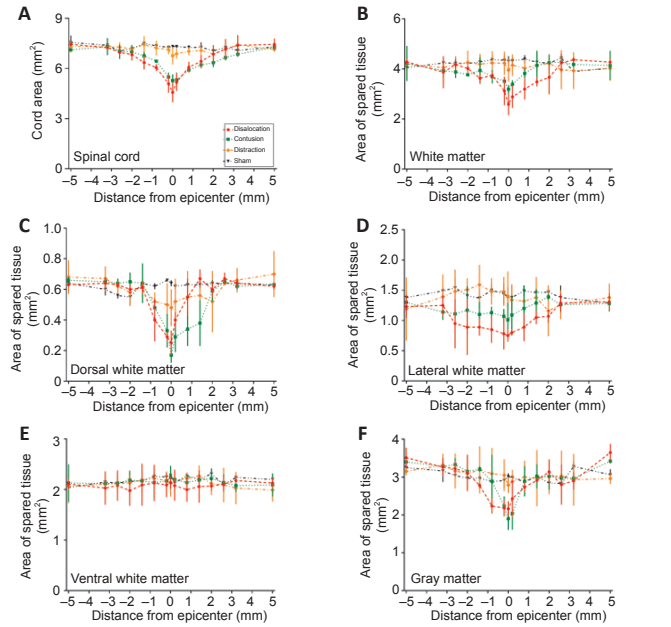

Figure 8 | Cross-sectional area of total spinal cord and spared tissue on Luxol fast blue-stained spinal cord sections.
The spinal cord was analyzed relative to the injury epicenter from −5 mm (rostral) to +5 mm (caudal). (A, B) Cross-sectional areas of the total spinal cord and total white matter were smaller in the contusion and dislocation groups than in the sham group. Tissue damage was greater in the dislocation group. (C) Compared with the control group, dorsal white matter area was smaller in the dislocation and contusion groups; area was particularly small in the contusion group caudal to the lesion site. (D) Lateral white matter area was lower around the epicenter in the dislocation and contusion groups than in the control group; area was particularly low in the dislocation group. (E) Ventral area of spared white matter did not differ between the sham group and any of the three spinal cord injury types. (F) Gray matter cross-sectional area was greater in the distraction injury group than in the dislocation and contusion injury groups; however, gray matter cross sectional area did not differ between the distraction injury and sham groups. Data shown are means ± standard deviation (n = 10 in each group) and were analyzed by two-way repeated-measures analysis of variance followed by Tukey's honestly significant difference testing.

Myelinated axon density

SMI312/myelin basic protein immunofluorescence staining showed that density of myelinated axons qualitatively differed among the three injury types and varied according to location. At the epicenter of injury in the gracile fasciculus of the contusion injury group, myelinated axon density was low and a cavity filled with myelin debris was observed; damage extended 5 mm caudally (**Figure 9A**). In the dislocation injury group, the degree of damage and cavitation was slightly lower. Although most axons at the epicenter were variably destroyed, most ascending sensory axons were preserved 3 and 5 mm rostral and caudal to the epicenter; partial sparing was observed as close as 1 mm from the epicenter (**Figure 9A**). The extent and distribution of damage differed in the distraction injury group, which showed a relative reduction in packing density of myelinated axons because of an increase in extracellular spaces (**Figure 9A**).

Similar patterns of myelinated axon injury were observed in the dorsal corticospinal tract. In the contusion and dislocation injury groups, approximately 10% to 50% of myelinated corticospinal axons were spared 3 mm proximal to the injury; few were spared at the epicenter, where myelin debris, tract interruption and cavitation were observed (**Figure 9B**). Many corticospinal axons were preserved at all locations in the distraction injury group. Both groups showed extensive degeneration of lateral white matter axons, a large amount of myelin debris, and many demyelinated axons (**Figure 10A**). Axon damage in the lateral white matter was limited to within 1 mm from the epicenter in the contusion and dislocation injury groups. Interestingly, ventral white matter damage was not observed in any of the three injury types (**Figure 10B**).

In the gracile fasciculus, few myelinated axons survived at the epicenter after contusion and dislocation injuries, particularly so for the dislocation injury group (**Figure 11A** and **B**). In the lateral white matter, axon damage was limited to within 1 mm of the epicenter in the contusion and dislocation injury groups; myelinated axon density was lower in the contusion group (**Figure 11C**). The distraction injury group did not show signs of lateral white matter damage. Furthermore, no differences were found in the ventral white matter between the three injury mechanisms (**Figure 11D**).

Correlation between evoked potentials and histological findings

Scatterplots of electrophysiological and histological findings are shown in **Figure 12**. SEP latency and amplitude significantly correlated with number of myelinated axons in the gracile fasciculus (r = –0.51 and 0.60, respectively; P = 0.0042 and 0.0031, respectively; **Figure 12A**). MEP latency significantly correlated with number of myelinated axons in the lateral (r = –0.46, P = 0.0302), dorsal (r = –0.62, P = 0.0335), and ventral (r = –0.45, P = 0.0062) white matter. MEP amplitude significantly correlated with number of myelinated axons in the lateral white matter (r = 0.66, P = 0.0191), but not in the corticospinal tract and ventral white matter (**Figure 12B**).

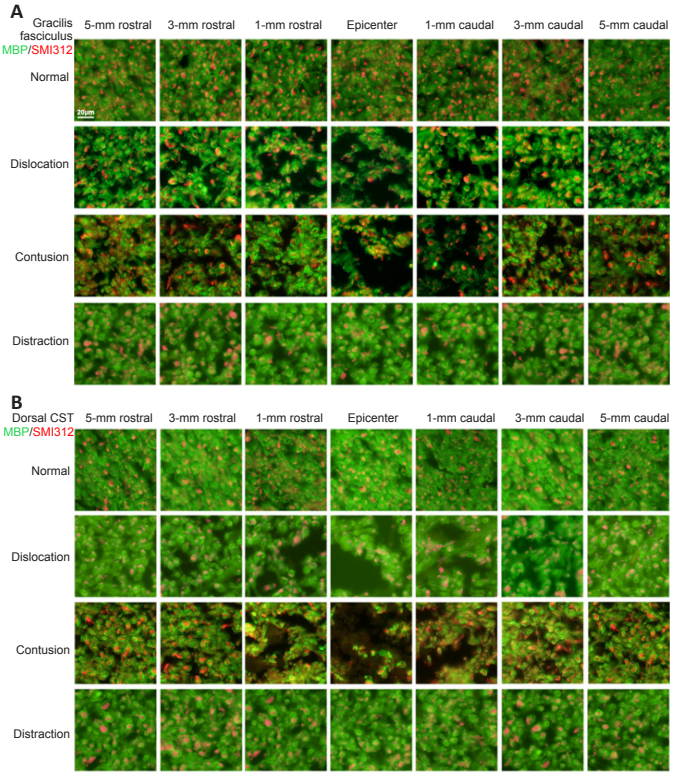

Figure 9 | Immunofluorescence micrographs of myelinated axons in the gracile fasciculus (A) and dorsal corticospinal tract (B) (CST).
Representative immunofluorescence imaging of regions of interest for quantitative analysis of white matter damage showing axons (SMI312$^+$, red, stained by DyLight 594) and myelin sheaths (MBP$^+$, green, stained by DyLight 488). Normal tracts show dense small myelinated axons in the gracile fasciculus (GF) and dorsal CST, typically with a green myelin ring surrounding a red axon in the middle. In contusion and dislocation injuries, both the gracile fasciculus and CST were destroyed and replaced by a cavity with extensive myelin fragments. At 3 and 5 mm from the epicenter, the proximal part of the ascending sensory axon mostly remained after dislocation and was partially spared 1 mm from the epicenter. After contusion injury, the injury extended up to 5 mm caudal to the epicenter. In contrast, the density of myelinated axons did not significantly change after distraction injury and many axons consistent with typical small corticospinal axons remained at all positions. Scale bar: 20 μm. MBP: Myelin basic protein.

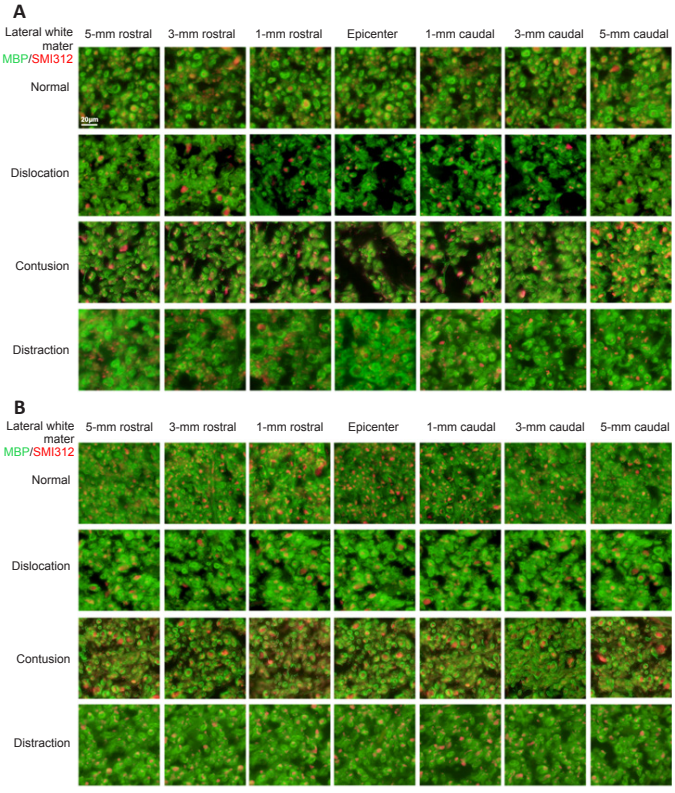

Figure 10 | Immunofluorescence micrographs of myelinated axons in the lateral white matter (A) and ventral white matter (B).
Representative immunofluorescence imaging of regions of interest for quantitative analysis of white matter damage showing axons (SMI312$^+$, red, stained by DyLight 594) and myelin sheaths (MBP$^+$, green, stained by DyLight 488). Normal tracts show dense small myelinated axons in the lateral and ventral white matter, typically with a green myelin ring surrounding a red axon in the middle. Lateral and ventral white matter show a red axon in the middle surrounded by a dense typical green myelin sheath. Contusion and dislocation injuries produced pronounced damage at the injury epicenter and further distally, while no significant damage was observed in the lateral and ventral white matter after distraction injury. Scale bar: 20 μm. MBP: Myelin basic protein.

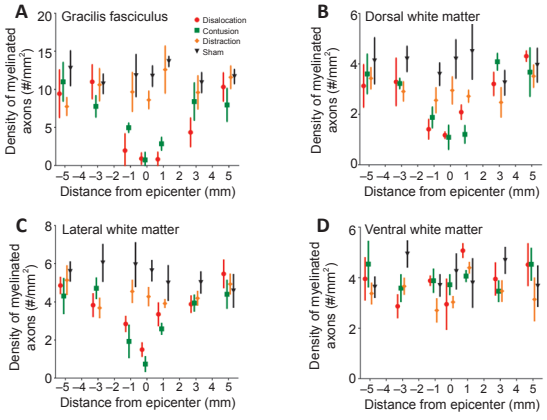

Figure 11 | Density of myelinated axons according to type of spinal cord injury.
(A) Density in the gracile fasciculus (i) differences from control: dislocation –1, to +3 mm; contusion –3 to +5 mm; distraction none (ii) differences between contusion and dislocation: –3, +3 mm. (B) Density in the dorsal corticospinal tract: (i) differences from control: contusion –3 to +1 mm; dislocation –5, –1 to +1 mm; distraction: none; (ii) differences between dislocation and contusion: –1 mm. (C) Density in the lateral white matter: (i) differences from control: dislocation-3 to +3 mm; contusion –5 to +3 mm; distraction none; (ii) differences between dislocation and contusion: –1, 0 mm. (D) No differences were found between the three injury types in the ventral white matter. Data shown are means ± standard deviation (n = 10 in each group). Data were analyzed using two-way repeated-measures analysis of variance followed by Tukey's honestly significant difference testing.

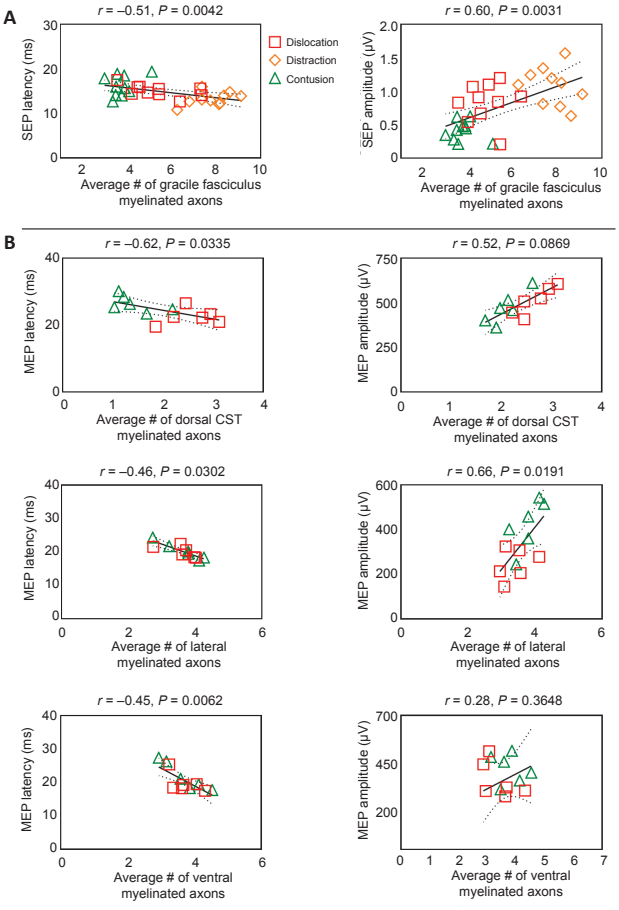

Figure 12 | Scatterplots showing the relationship between electrophysiological and immunofluorescence outcomes using Pearson's correlation analysis.
The linear regression line of the best fit is represented by a solid line. The 95% confidence interval is represented by a dotted line.

Discussion

SCI during spinal surgery occurs insidiously and has various causes. Early and accurate neurophysiological identification of injury type is challenging but important (Guo et al., 2021). Our study is based on the rationale that different modes of SCI will lead to different pathological changes in the spinal cord and induce distinct sensory and motor signal responses via separate neural pathways. Moreover, identification of these signal response changes is the basis for identifying different SCI types. We compared electrophysiological and histological findings between dislocation, contusion, and distraction types of SCI and demonstrated distinct differences in SEPs, MEPs, and primary histological changes. Contusion caused the greatest rostrocaudal extent of tissue injury and was associated with significantly attenuated SEP and MEP responses. Dislocation resulted in the greatest overall loss of white matter tissue, particularly in the lateral white matter, as well as a greater reduction in MEP responses than contusion. Although enlarged extracellular spaces were observed without substantial structural alteration following distraction injury, SEP responses slightly decreased and MEP responses were lost. Furthermore, histological and electrophysiological findings were correlated. These results demonstrate the complex and varied electrophysiologic and histopathologic effects of SCI and reveal the potential value of SEPs and MEPs in diagnosing and identifying intraoperative SCI type.

Spinal deformities often require manual correction, which carries a risk of iatrogenic SCI. The type of injury varies according to cause. Spinal cord dislocation often occurs in osteoporotic patients with kyphotic deformity, who are at risk of postoperative fracture and dislocation (Ruf et al., 2006). Contusion may occur due to errant bone screw placement (Safain et al., 2014). Distraction injury may result from overstretching during scoliosis correction (Sawyer et al., 2016). Therefore, early diagnosis and necessary measures are essential before neurological deficit occurs. The three SCI types examined in our study exhibited a series of deformation patterns in the spinal cord that were related to electrophysiological differences. Contused animals showed the greatest deterioration in SEP and MEP responses, with prolonged latency and reduced amplitude; furthermore, compared with animals with dislocation or distraction injuries, contused animals showed the least sparing of myelinated axons in the dorsal white matter. Dislocation injury caused the greatest loss in number of myelinated axons, particularly in the lateral white matter. Also in this type, signal changes were larger in MEP responses than SEP responses: SEP amplitude was only partially reduced, whereas MEP latency was prolonged and amplitude was reduced. Distraction injury caused virtually no spinal cord tissue damage, although SEP responses were attenuated and MEP responses abolished. These findings are similar to those reported in a study of electrophysiological monitoring during spinal scoliosis surgery. In that study, after mechanical distraction was applied, MEP response threshold voltage significantly increased followed by a complete loss of motor responses; however, SEP responses did not change (Lyon et al., 2004). The discrepancy between histologic and electrophysiologic findings may be attributed to transient ischemia induced by spinal microcirculation block

without structural axonal disruption (Kawahara et al., 2005; Kato et al., 2008). This emphasizes the predictive value of electrophysiological assessment, in which MEPs are more sensitive to distraction SCI than SEPs. This, along with our results, indicate that SCI type affects both spinal cord histopathology and electrophysiology.

In theory, contusion and dislocation injuries produce localized compressive and high lateral tensile strain on the spinal cord, while the strain caused by distraction is more uniformly distributed and has a lower peak (Li and Dai, 2009; Russell et al., 2012; Mihara et al., 2018; Ma et al., 2019; Guo et al., 2020; Huang et al., 2021). In our study, both dislocation and contusion injuries caused tissue damage and loss along the rostrocaudal axis of the injured spinal cord and contusion injuries resulted in maximal loss of myelinated axons in the dorsal white matter. Although we observed no obvious acute white matter tissue damage or degenerative changes after distraction injury, a previous study reported detection of substantial spinal cord damage 8 weeks after injury that was characterized by a large degree of central destruction and far-ranging demyelination throughout all levels of the spinal cord (Chen et al., 2016). Therefore, long-term follow-up examination after experimental injury is vital to fully evaluate the effect of various injury types.

Hemorrhage is often used as an indicator of primary injury because it plays an important role in the initiation of subsequent neuropathological events (Losey et al., 2014; Okada, 2016; Ellingson et al., 2019). In a rat SCI model, Choo et al. found that contusion and dislocation injuries caused similar central damage to the gray matter vascular system and similarly localized increased membrane permeability 5 minutes after injury; however no obvious hemorrhage was observed after distraction. Furthermore, both injury-related ischemia and inflammatory cell infiltration contribute to free radical generation and oxidative stress, which exacerbates cellular damage (Kwon et al., 2010; Jiang et al., 2016; Li et al., 2019; Huang et al., 2020). The time window for treatment of distraction injury may be longer because it causes less hemorrhage. In agreement, our results showed that contusion and dislocation injuries caused hemorrhage in the gray matter and distraction injuries caused only minor focal hemorrhage. Hemorrhage and hemorrhagic necrosis increase with injury severity (Lau et al., 2013; Mondello et al., 2015). However, our study focused on the association of electrophysiological testing with injury type rather than severity. Because SEPs and MEPs disappear in several injury types, severity of injury induced in this study was set to mild-to-moderate based on previous models (Dabney et al., 2004; Fiford et al., 2004; Jin et al., 2014).

Because animals were sacrificed soon after SCI owing to ethical considerations, progression of secondary degeneration and convergence/divergence of injury patterns was not assessed. However, biomechanical injury was the variable prioritized and it was necessary to sacrifice animals early to assess spatial distribution of injury and electrophysiological changes without confounding secondary events. Furthermore, early sacrifice precluded long-term assessment of spinal cord damage. A better experimental design with restricted injury severity control and post-injury examination should be investigated in a future study.

This study showed that spinal cord tissue damage differs between contusion, dislocation, and distraction types of SCI. These injury types exhibit distinct SEP and MEP changes that significantly correlate with their different histologic findings. Patterns of electrophysiologic changes in combination with SEPs and MEPs have the potential to indicate the type of SCI during surgery, which can guide appropriate treatment.

Author contributions: *Study conception and design, manuscript review and edit: YH; experimental implementation: RL, HLL, HYC; data analysis/interpretation: YCH; manuscript writing: RL. All authors contributed to this study and approved the final manuscript.*
Conflicts of interest: *The authors declare that they have no conflict of interest.*
Availability of data and materials: *All data generated or analyzed during this study are included in this published article and its supplementary information files.*

Additional file:
Additional file 1: *Electrophysiological signal changes in animals of the three groups.*

References

Chen K, Liu J, Assinck P, Bhatnagar T, Streijger F, Zhu Q, Dvorak MF, Kwon BK, Tetzlaff W, Oxland TR (2016) Differential histopathological and behavioral outcomes eight weeks after rat spinal cord injury by contusion, dislocation, and distraction mechanisms. J Neurotrauma 33:1667-1684.
Chen X, Li H (2022) Neuronal reprogramming in treating spinal cord injury. Neural Regen Res 17:1440-1445.
Choi EH, Gattas S, Brown NJ, Hong JD, Limbo JN, Chan AY, Oh MY (2021) Epidural electrical stimulation for spinal cord injury. Neural Regen Res 16:2367-2375.
Choo AM, Liu J, Lam CK, Dvorak M, Tetzlaff W, Oxland TR (2007) Contusion, dislocation, and distraction: primary hemorrhage and membrane permeability in distinct mechanisms of spinal cord injury. J Neurosurg Spine 6:255-266.
Choo AM, Liu J, Dvorak M, Tetzlaff W, Oxland TR (2008) Secondary pathology following contusion, dislocation, and distraction spinal cord injuries. Exp Neurol 212:490-506.
Choo AM, Liu J, Liu Z, Dvorak M, Tetzlaff W, Oxland TR (2009) Modeling spinal cord contusion, dislocation, and distraction: characterization of vertebral clamps, injury severities, and node of Ranvier deformations. J Neurosci Methods 181:6-17.
Dabney KW, Ehrenshteyn M, Agresta CA, Twiss JL, Stern G, Tice L, Salzman SK (2004) A model of experimental spinal cord trauma based on computer-controlled intervertebral distraction: characterization of graded injury. Spine (Phila Pa 1976) 29:2357-2364.
Ellingson BM, Woodworth DC, Leu K, Salamon N, Holly LT (2019) Spinal cord perfusion MR imaging implicates both ischemia and hypoxia in the pathogenesis of cervical spondylosis. World Neurosurg 128:e773-781.
Fiford RJ, Bilston LE, Waite P, Lu J (2004) A vertebral dislocation model of spinal cord injury in rats. J Neurotrauma 21:451-458.
Ghasem-Zadeh A, Galea MP, Nunn A, Panisset M, Wang XF, Iuliano S, Boyd SK, Forwood MR, Seeman E (2021) Heterogeneity in microstructural deterioration following spinal cord injury. Bone 142:115778.
Guo X, Xue Q, Zhao J, Yang Y, Yu Y, Liu D, Liu J, Yang W, Mu L, Zhang P, Wang T, Han H, Liu S, Zhu Y, Wang T, Qu C; On behalf of Chinese Association of Neurorestoratology (Preparatory) and China Committee of International Association of Neurorestoratology (2020) Clinical diagnostic and therapeutic guidelines of stroke neurorestoration (2020 China version). J Neurorestoratol 8:241-251.
Guo X, Feng Y, Sun T, Feng S, Tang J, Chen L, Cao X, Lin H, He X, Li M, Zhang Z, Yin G, Mei X, Huang H (2021) Clinical guidelines for neurorestorative therapies in spinal cord injury (2021 China version). J Neurorestoratol 9:31-49.
Howell K, Hopkins N, McLoughlin P (2002) Combined confocal microscopy and stereology: a highly efficient and unbiased approach to quantitative structural measurement in tissues. Exp Physiol 87:747-756.
Hu Y, Wen CY, Li TH, Cheung MM, Wu EX, Luk KD (2011) Somatosensory-evoked potentials as an indicator for the extent of ultrastructural damage of the spinal cord after chronic compressive injuries in a rat model. Clin Neurophysiol 122:1440-1447.
Huang H, Chen L, Mao G, Sharma HS (2020) Clinical neurorestorative cell therapies: developmental process, current state and future prospective. J Neurorestoratol 8:61-82.
Huang H, Chen L, Chopp M, Young W, Bach JR, He X, Sarnowaska A, Xue M, Zhao RC, Shetty A, Siniscalco D, Guo X, Khoshnevisan A, Hawamdeh Z (2021) The 2020 yearbook of neurorestoratology. J Neurorestoratol 9:1-12.
Huang Z, Li R, Liu J, Huang Z, Hu Y, Wu X, Zhu Q (2018) Longitudinal electrophysiological changes after cervical hemi-contusion spinal cord injury in rats. Neurosci Lett 664:116-122.
Jiang W, Li M, He F, Bian Z, Liu J, He Q, Wang X, Sun T, Zhu L (2016) Dopamine D1 receptor agonist A-68930 inhibits NLRP3 inflammasome activation and protects rats from spinal cord injury-induced acute lung injury. Spinal Cord 54:951-956.
Jin Y, Bouyer J, Haas C, Fischer I (2014) Behavioral and anatomical consequences of repetitive mild thoracic spinal cord contusion injury in the rat. Exp Neurol 257:57-69.
Kakinohana M, Nakamura S, Fuchigami T, Sugahara K (2007) Transcranial motor-evoked potentials monitoring can detect spinal cord ischemia more rapidly than spinal cord-evoked potentials monitoring during aortic occlusion in rats. Eur Spine J 16:787-793.
Kato S, Kawahara N, Tomita K, Murakami H, Demura S, Fujimaki Y (2008) Effects on spinal cord blood flow and neurologic function secondary to interruption of bilateral segmental arteries which supply the artery of Adamkiewicz: an experimental study using a dog model. Spine (Phila Pa 1976) 33:1533-1541.
Kawahara N, Tomita K, Kobayashi T, Abdel-Wanis ME, Murakami H, Akamaru T (2005) Influence of acute shortening on the spinal cord: an experimental study. Spine (Phila Pa 1976) 30:613-620.
Kwon BK, Stammers AM, Belanger LM, Bernardo A, Chan D, Bishop CM, Slobogean GP, Zhang H, Umedaly H, Giffin M, Street J, Boyd MC, Paquette SJ, Fisher CG, Dvorak MF (2010) Cerebrospinal fluid inflammatory cytokines and biomarkers of injury severity in acute human spinal cord injury. J Neurotrauma 27:669-682.
Lau NS, Gorrie CA, Chia JY, Bilston LE, Clarke EC (2013) Severity of spinal cord injury in adult and infant rats after vertebral dislocation depends upon displacement but not speed. J Neurotrauma 30:1361-1373.
Li XF, Dai LY (2009) Three-dimensional finite element model of the cervical spinal cord: preliminary results of injury mechanism analysis. Spine (Phila Pa 1976) 34:1140-1147.
Li Z, Wu F, Xu D, Zhi Z, Xu G (2019) Inhibition of TREM1 reduces inflammation and oxidative stress after spinal cord injury (SCI) associated with HO-1 expressions. Biomed Pharmacother 109:2014-2021.
Losey P, Young C, Krimholtz E, Bordet R, Anthony DC (2014) The role of hemorrhage following spinal-cord injury. Brain Res 1569:9-18.
Lyon R, Lieberman JA, Grabovac MT, Hu S (2004) Strategies for managing decreased motor evoked potential signals while distracting the spine during correction of scoliosis. J Neurosurg Anesthesiol 16:167-170.
Ma C, Zhang P, Shen Y (2019) Progress in research into spinal cord injury repair: tissue engineering scaffolds and cell transdifferentiation. J Neurorestoratol 7:196-206.
MacDonald DB, Dong C, Quatrale R, Sala F, Skinner S, Soto F, Szelényi A (2019) Recommendations of the International Society of Intraoperative Neurophysiology for intraoperative somatosensory evoked potentials. Clin Neurophysiol 130:161-179.
Mattucci S, Speidel J, Liu J, Ramer MS, Kwon BK, Tetzlaff W, Oxland TR (2019) Development of a traumatic cervical dislocation spinal cord injury model with residual compression in the rat. J Neurosci Methods 322:58-70.
Mihara A, Kanchiku T, Nishida N, Tagawa H, Ohgi J, Suzuki H, Imajo Y, Funaba M, Nakashima D, Chen X, Taguchi T (2018) Biomechanical analysis of brachial plexus injury: availability of three-dimensional finite element model of the brachial plexus. Exp Ther Med 15:1989-1993.
Mondello SE, Sunshine MD, Fischedick AE, Moritz CT, Horner PJ (2015) A cervical hemi-contusion spinal cord injury model for the investigation of novel therapeutics targeting proximal and distal forelimb functional recovery. J Neurotrauma 32:1994-2007.
Morris SH, Howard JJ, El-Hawary R (2017) Comparison of motor-evoked potentials versus somatosensory-evoked potentials as early indicators of neural compromise in rat model of spinal cord compression. Spine (Phila Pa 1976) 42:E326-E331.
Nuwer MR, Schrader LM (2019) Spinal cord monitoring. Handb Clin Neurol 160:329-344.
Okada S (2016) The pathophysiological role of acute inflammation after spinal cord injury. Inflamm Regen 36:20.
Ruf M, Rehm S, Poeckler-Schoeniger C, Merk HR, Harms J (2006) Iatrogenic fractures in ankylosing spondylitis--a report of two cases. Eur Spine J 15:100-104.
Russell CM, Choo AM, Tetzlaff W, Chung TE, Oxland TR (2012) Maximum principal strain correlates with spinal cord tissue damage in contusion and dislocation injuries in the rat cervical spine. J Neurotrauma 29:1574-1585.
Safain MG, Hwang S, King J, Cahill P, Samdani A (2014) Loss of correction in spinal cord injury-related scoliosis after pedicle screw fixation. Childs Nerv Syst 30:673-680.
Sawyer JR, de Mendonça RG, Flynn TS, Samdani AF, El-Hawary R, Spurway AJ, Smith JT, Emans JB, St Hilaire TA, Soufleris SJ, Murphy RP (2016) Complications and radiographic outcomes of posterior spinal fusion and observation in patients who have undergone distraction-based treatment for early onset scoliosis. Spine Deform 4:407-412.
Schneider CA, Rasband WS, Eliceiri KW (2012) NIH Image to ImageJ: 25 years of image analysis. Nat Methods 9:671-675.
Schumacher PA, Siman RG, Fehlings MG (2000) Pretreatment with calpain inhibitor CEP-4143 inhibits calpain I activation and cytoskeletal degradation, improves neurological function, and enhances axonal survival after traumatic spinal cord injury. J Neurochem 74:1646-1655.
Tator CH (2006) Review of treatment trials in human spinal cord injury: issues, difficulties, and recommendations. Neurosurgery 59:957-982; discussion 982-987.
Tian T, Li XG (2021) Problems and challenges in regeneration and repair of spinal cord injury. Zhongguo Zuzhi Gongcheng Yanjiu 25:3039-3048.
Walker CL, Zhang YP, Liu Y, Li Y, Walker MJ, Liu NK, Shields CB, Xu XM (2016) Anatomical and functional effects of lateral cervical hemicontusion in adult rats. Restor Neurol Neurosci 34:389-400.
Wang Y, Cui H, Pu J, Luk KD, Hu Y (2015) Time-frequency patterns of somatosensory evoked potentials in predicting the location of spinal cord injury. Neurosci Lett 603:37-41.

C-Editor: Zhao M; S-Editors: Yu J, Li CH; L-Editors: Yu J, Song LP; T-Editor: Jia Y